Key Engineering Materials
ISSN: 1662-9795, Vol. 1021, pp 7-15
doi:10.4028/p-47sFxF

Submitted: 2024-09-19
Revised: 2025-08-06
Accepted: 2025-08-06
Online: 2025-09-05

Investigation on Effect of Electrical Characteristics of Proton Implanted 4H-SiC MOSFET

Naoki Shikama[1,a *], Kazuya Ishibashi[1,b], Hiroki Niwa[2,c], Takanori Tanaka[1,d], Hiroyuki Amishiro[2,e], Akifumi Imai[2,f], Katsutoshi Sugawara[2,g], Yasuhiro Kagawa[1,h] and Akihiko Furukawa[1,i]

[1]Power Device Works, Mitsubishi Electric Corporation,1-1-1 Imajuku-higashi, Nishi-ku, Fukuoka-shi, Fukuoka, 819-0192, Japan

[2]Advanced Technology R&D Center, Mitsubishi Electric Corporation, 8-1-1 Tsukaguchi-honmachi, Amagasaki-shi, Hyogo, 661-8661, Japan

[a]Shikama.Naoki@df.MitsubishiElectric.co.jp, [b]Ishibashi.Kazuya@ak.MitsubishiElectric.co.jp, [c]Niwa.Hiroki@dp.MitsubishiElectric.co.jp, [d]Tanaka.Takanori@cb.MitsubishiElectric.co.jp, [e]Amishiro.Hiroyuki@cb.MitsubishiElectric.co.jp, [f]Imai.Akifumi@ys.MitsubishiElectric.co.jp, [g]Sugawara.Katsutoshi@ea.MitsubishiElectric.co.jp, [h]Kagawa.Yasuhiro@cj.MitsubishiElectric.co.jp, [i]Furukawa.Akihiko@df.MitsubishiElectric.co.jp

Keywords: MOSFET, body diode, bipolar degradation, proton implantation, electrical characteristics

Abstract. We investigated how proton implantation influences electrical characteristics of the 4H-SiC MOSFETs. Bipolar degradation in SiC is one of the key issues to be solved for utilizing the bipolar operation in SiC power devices. Its suppression with the proton implantation technique has recently been reported. If we can apply such a new technique being involved for realizing reliable SiC MOSFETs, it would give us great merit to take advantage of the body diode. However, few study has been reported of proton implanted SiC MOSFETs, to our knowledge. Thus, we fabricated 4,000 chips, applied current stress to their body diodes and subsequently evaluated them to verify statistically any effectiveness on the suppression of the bipolar degradation as well as on the electrical performance of MOSFET in order to consider its technological applicability to their mass production process. We found that proton implantation not only has little influence on the static electrical characteristics of the MOSFETs but also improves the switching characteristics.

Introduction

Silicon carbide (SiC) is the candidate as an alternative material for Si in switching applications. An external Schottky barrier diode (SBD) has been used as a free-wheeling diode in anti-parallel configuration with a MOSFET in designing typical switching applications. Body diode has also been widely recognized and utilized as free-wheeling diode instead of SBD to realize cost reduction and shrinkage of the systems comprising of the SiC power devices.

Bipolar degradation in SiC is one of the key issues to be solved for utilizing the bipolar operation in SiC power devices like a body diode. The recombination energy of electron-hole pairs in the bipolar operation mode expands the stacking faults (SFs) from basal plane dislocations (BPDs). The typical method for its prevention has been reported [1] by using a heavily N-doped SiC epitaxial buffer layer. However, such a layer requires precise control of its thickness and uniform impurity doping throughout the wafer, which are often challenging. Therefore, there has been a need to establish any other methods for overcoming this troublesome issue.

It has been recently reported that the suppression of the expansion of the SFs could be realized by H^+ (proton) implantation [2-4]. The proton implantation as much as 1×10^{11} cm^{-2} or more was shown to be effective. If we can apply such a new technique for the fabrication of the SiC MOSFETs, it would provide the way to take advantage of the body diode in the SiC MOSFET. It is important to verify that proton does not have a side effect on the electrical characteristics of the MOSFET.

However, few study has been reported on fabrication of proton implanted SiC MOSFETs, to our knowledge. Thus, we fabricated huge numbers (about 4,000 chips) of MOSFETs, applied current stress to their body diodes and evaluated them to discuss possibility for the mass production and verify the bipolar degradation statistically.

Method

Figs. 1 (a) and (b) show the cross-sectional schematic of the SiC MOSFETs with and without proton implanted layer. We used n-type 4H-SiC wafers with an epitaxial conversion layer which was grown to convert BPDs to threading edge dislocations (TEDs), and a drift layer whose thickness was 12 μm. The off-cut angle of the wafer was 4°. Fig. 2 shows an experimental flow chart of the device fabrication and evaluation processes. It should be noted that the proton implantation was performed before the activation annealing process. The dose of proton are 1×10^{12} cm^{-2}, 1×10^{13} cm^{-2} and 1×10^{14} cm^{-2}. We also fabricated MOSFETs without proton for comparison. Number of the total measured chips was about 4,000. After the device fabrication, continuous current stress (typically, V_{GS} = 0 V, t = 2 min, T = 150°C and J_{SD} = 420 A/cm^2) was applied to the body diodes to evaluate the prevention of the expansion of the SFs on the bipolar degradation. Typical one chip data were plotted for each condition in the following Figs. 3-6 since all measured samples showed the same trend.

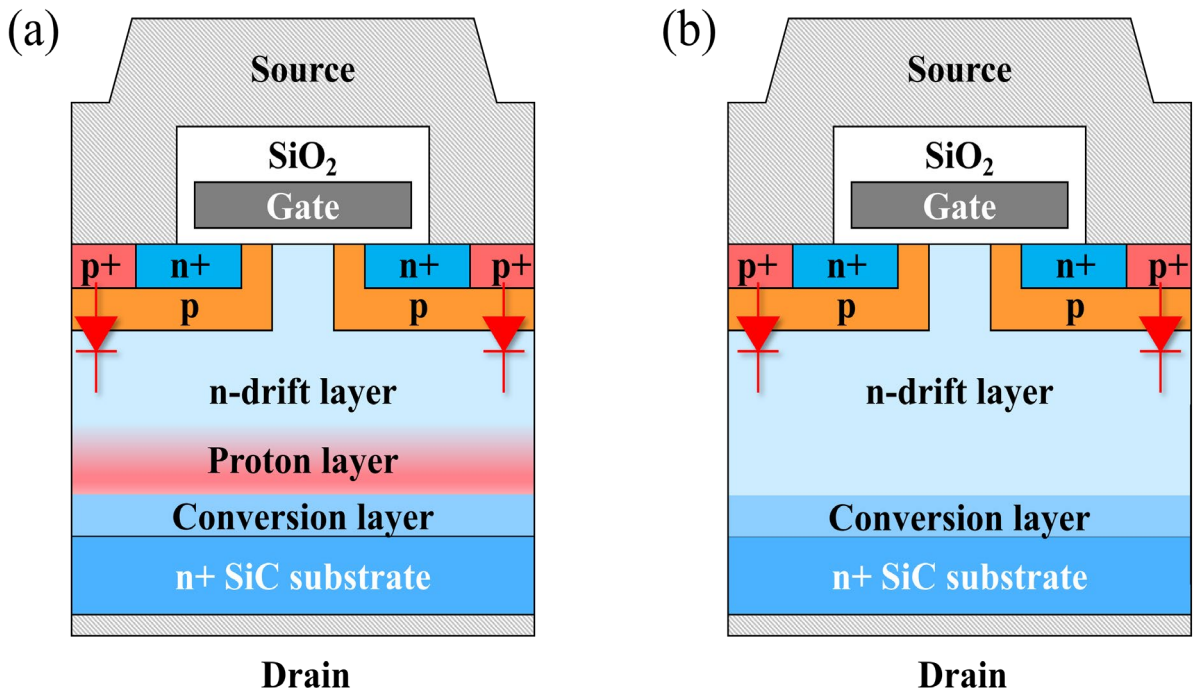

Fig. 1. Schematics of SiC MOSFETs (a) with proton implanted layer and (b) without proton implanted layer.

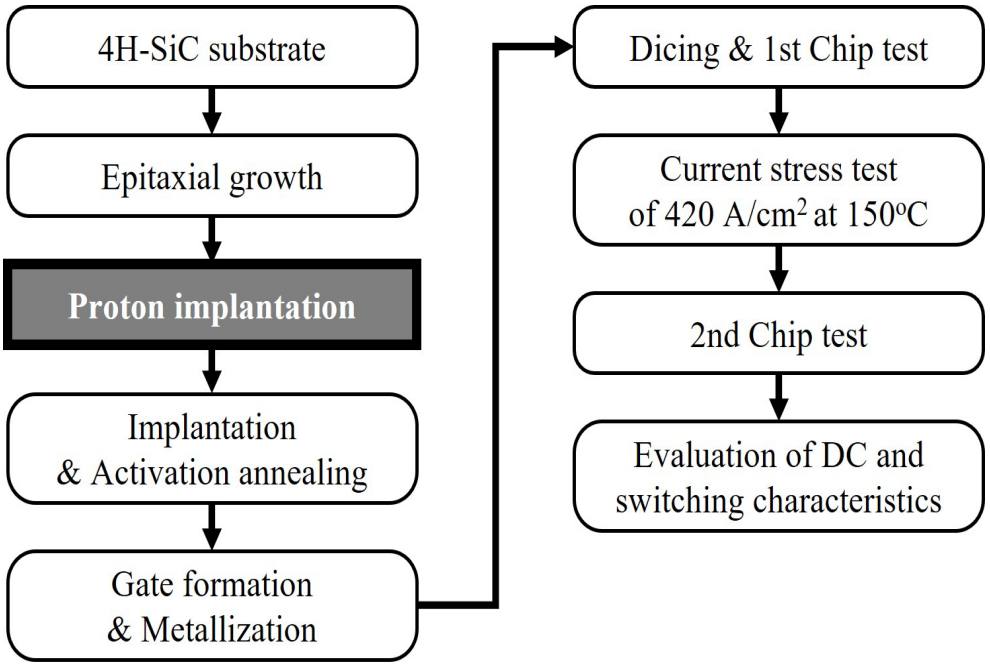

Fig. 2. Flow chart of the experiment.

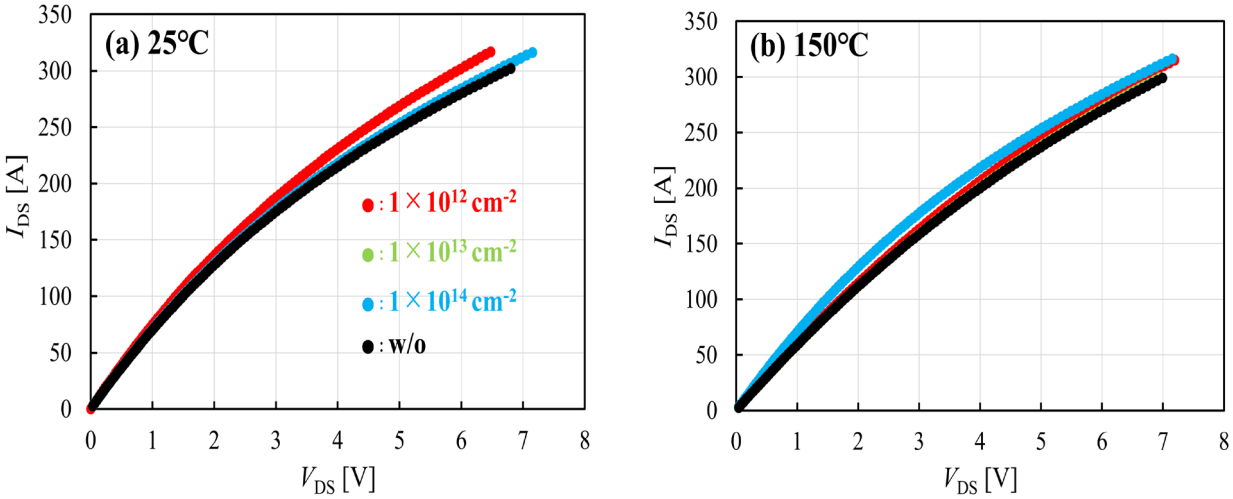

Fig. 3. I_{DS}-V_{DS} characteristics for the SiC MOSFETs with various proton dose of V_{GS} = +22 V (a) at 25°C and (b) at 150°C. I_{DS} and V_{DS} denote drain-source current and drain-source voltage, respectively.

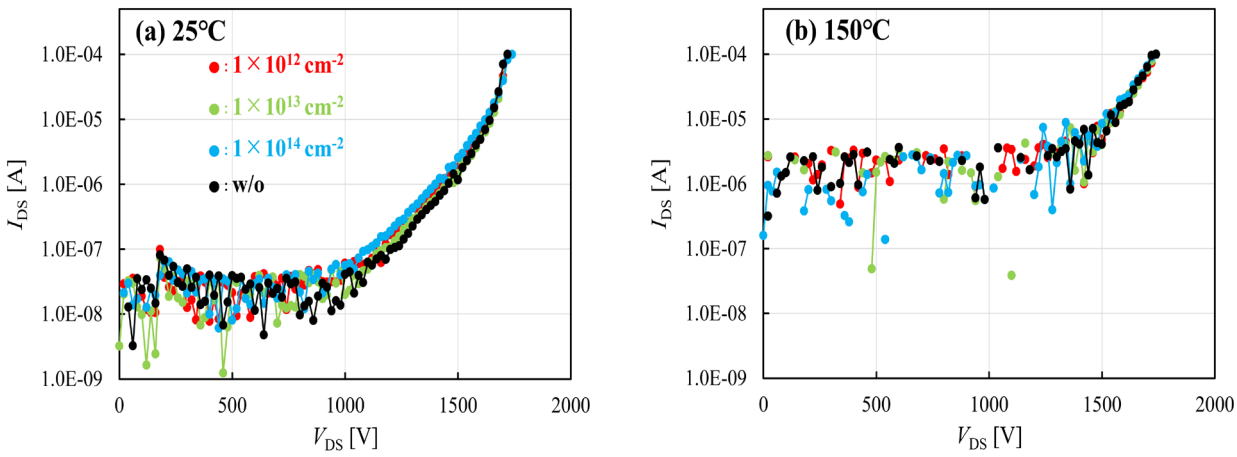

Fig. 4. I_{DS}-V_{DS} characteristics for the SiC MOSFETs with various proton dose of $V_{GS} = -10$ V (a) at 25°C and (b) at 150°C.

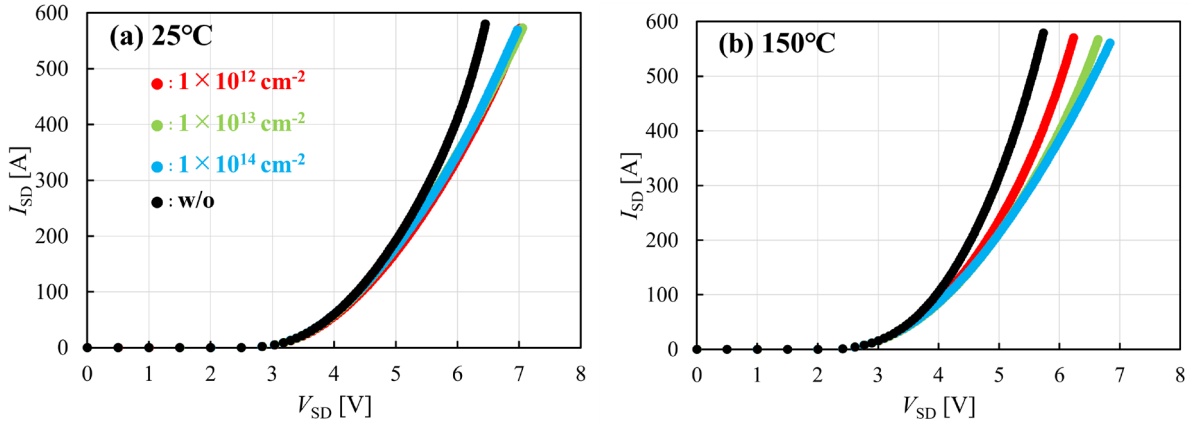

Fig. 5. I_{SD}-V_{SD} characteristics for the SiC MOSFETs with various proton dose of $V_{GS} = -10$ V (a) at 25°C and (b) at 150°C. I_{SD} and V_{SD} denote source-drain current and source-drain voltage, respectively.

Results and Discussion

Figs. 3 (a) and (b) show the output characteristics of the MOSFETs measured at 25°C and 150°C, respectively. All the curves are almost overlapped, which indicates the output characteristics of the MOSFET with proton is compatible to that without proton. Figs. 4 (a) and (b) show the drain-source leakage characteristics of the SiC MOSFETs measured at 25°C and 150°C, respectively. The increase of the leakage current due to proton implantation is not observed. Figs. 5 (a) and (b) show the 3rd quadrant characteristics of the SiC MOSFETs measured at 25°C and 150°C, respectively. Although all the samples operated as body diodes properly, their behavior is slightly different. At room temperature, differential on-resistance of the samples with proton, as a whole, is higher than that of the sample without proton (Fig. 5 (a)).

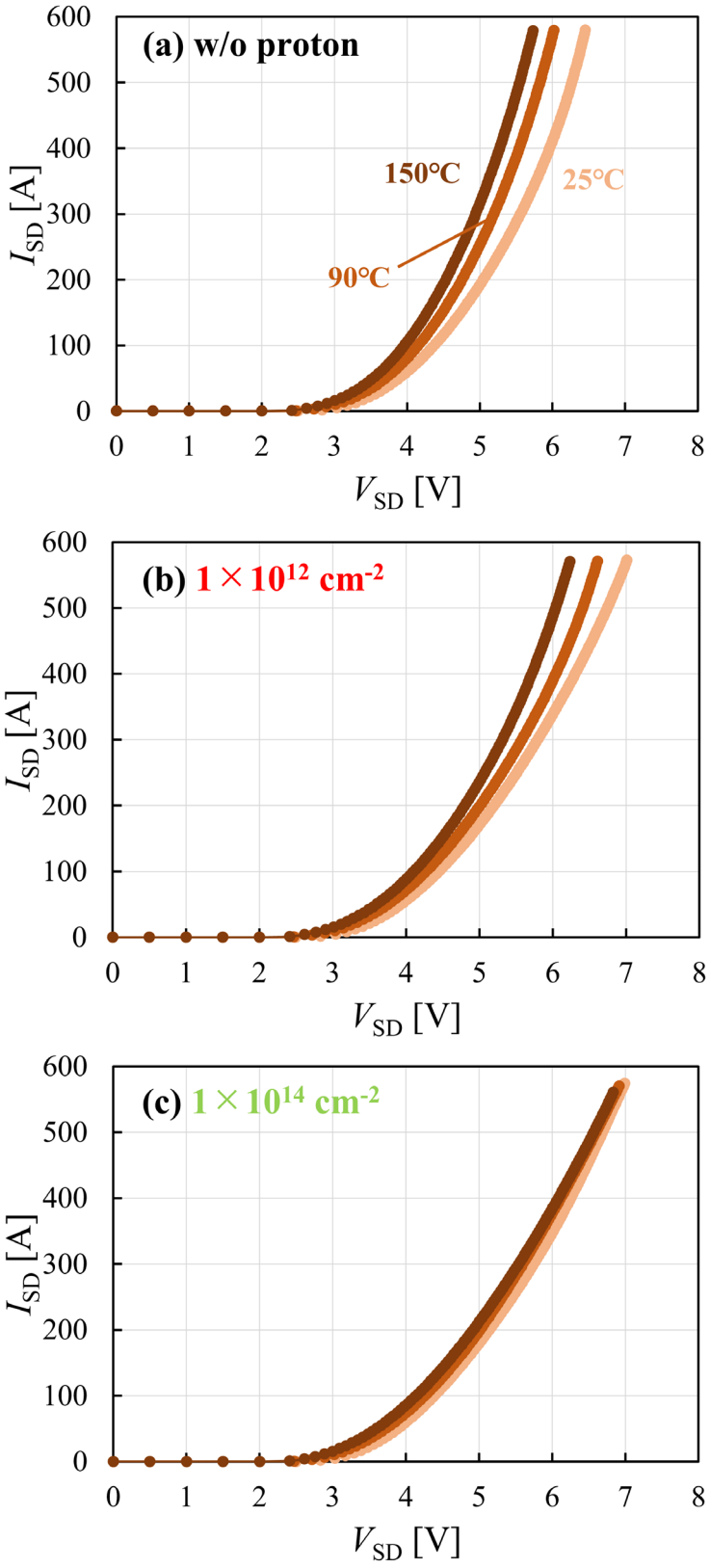

Fig. 6. I_{SD}-V_{SD} characteristics for the SiC MOSFETs of V_{GS} = −10 V (a) without proton, (b) with a proton dose of 1×10^{12} cm^{-2} and (c) with a proton dose of 1×10^{14} cm^{-2}, respectively. The data of Figs. 5 are replotted from the view of the temperature dependence.

At high temperature, quantitative difference between the samples with proton in the 3rd quadrant characteristics is clearly observed (Fig. 5 (b)), which implies that the effect of the proton is remarkable with the increasing of dose. Here, we suppose that the increase of the differential on-resistance of the samples with proton in the 3rd quadrant characteristics is insignificant as a switching device. It hardly affects the total loss because a body diode is conducted only in the dead time under normal pulse width modulation (PWM) operations. Figs. 6 (a)-(c) show the 3rd quadrant characteristics of the MOSFETs at each proton dose. The body diode without proton shows increase of the current as the temperature increases (Fig. 6 (a)). However, as the dose of proton increases, such an increase of the current is shown to gradually suppressed. Particularly, temperature dependence was almost suppressed with a proton dose of 1×10^{14} cm^{-2} (Fig. 6 (c)). Generally, more forward current flows at high temperature than at room temperature due to two effects:(i) the increase of the carrier density (particularly, minority carrier density) and (ii) the reduction of forward voltage (V_F) derived from the suppression of the potential barrier. As shown in Figs. 5 (a) and (b), the voltage, where current begins to flow, hardly depends on the dose of proton at each temperature. It implies that the latter effect is not suppressed, and the former effect is suppressed by proton implantation. This will be discussed later.

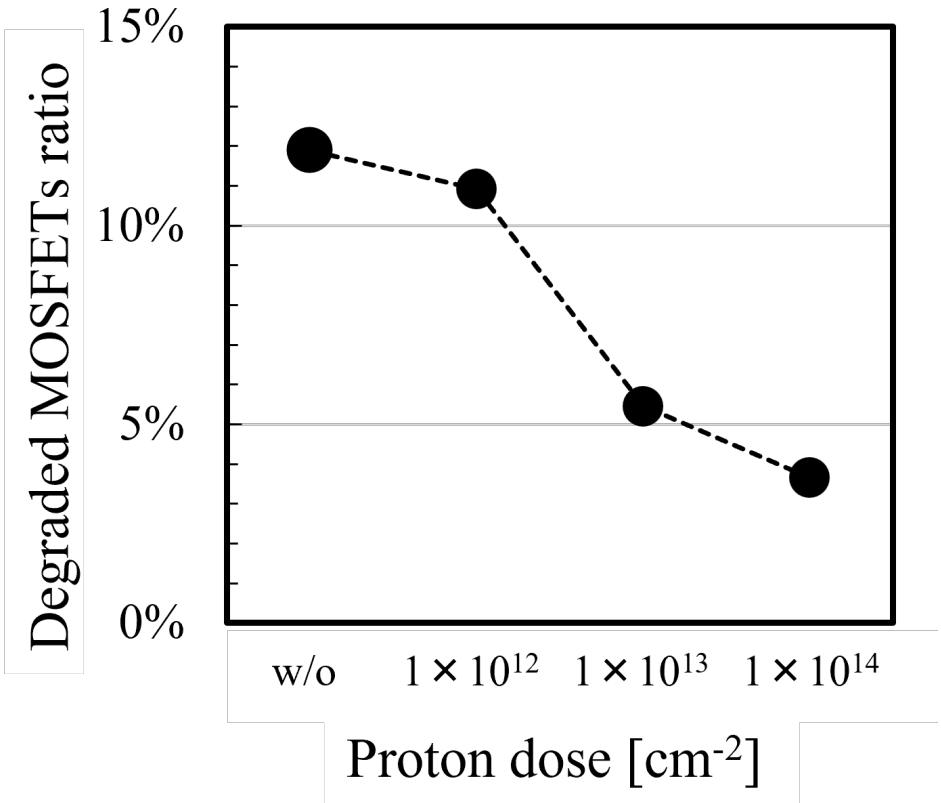

Fig. 7. The ratio of the degraded MOSFETs after current stress in each proton condition. The numbers of the tested samples are 1270 (w/o), 880 (1×10^{12} cm^{-2}), 844 (1×10^{13} cm^{-2}) and 823 (1×10^{14} cm^{-2}), respectively.

It is well known that the expansion of the SFs in the bipolar operation induces the increase of on-resistance of the MOSFET [5]. We evaluated how the on-resistance of MOSFET changed by the current stress on the body diode (Fig. 7). We defined the samples as “degraded” ones whose on-resistance increased over 3% after the current stress. The ratio of the degraded MOSFETs is inclined to show lower value with increasing the dose of proton, which is consistent with the previous report that claims suppression of the expansion of SFs by proton implantation [2]. With a proton dose of 1×10^{13} cm^{-2}, degraded MOSFET ratio becomes about 5%, which is the half value of that without proton. This result suggests that the bipolar degradation would be more suppressed by further increase

in the proton dose. Here, it was reported that proton of more than 10^{14} cm^{-2} hardly decreases the SFs density [2], which implies that proton of 1×10^{14} cm^{-2} might be enough to prevent the SFs from being expanded.

We also evaluated switching characteristics of the body diode. Figs. 8 (a) and (b) show the reverse recovery characteristics of the body diode with and without proton at 150°C. The switching characteristics were measured with the double pulse testing method, and the supply voltage and switching drain-source current are 760 V and 380A, respectively. The gate voltage of the upper arm and the lower arm are −5 V and −5/+22 V, respectively. The I_{DS} of the sample without proton reaches zero at about 0.42 μs and clear surge voltage was observed. By implanting proton, I_{DS} of the sample with 1×10^{14} cm^{-2} proton reaches almost zero at 0.4 μs, and the surge voltage became vague. Reverse recovery charge (Q_{rr}) and surge voltage increase (ΔV) are defined as follows,

$$Q_{rr} = -\int_{t_0}^{t_1} I_{DS}\, dt \tag{1}$$

$$\Delta V = V_{peak} - V_0 \tag{2}$$

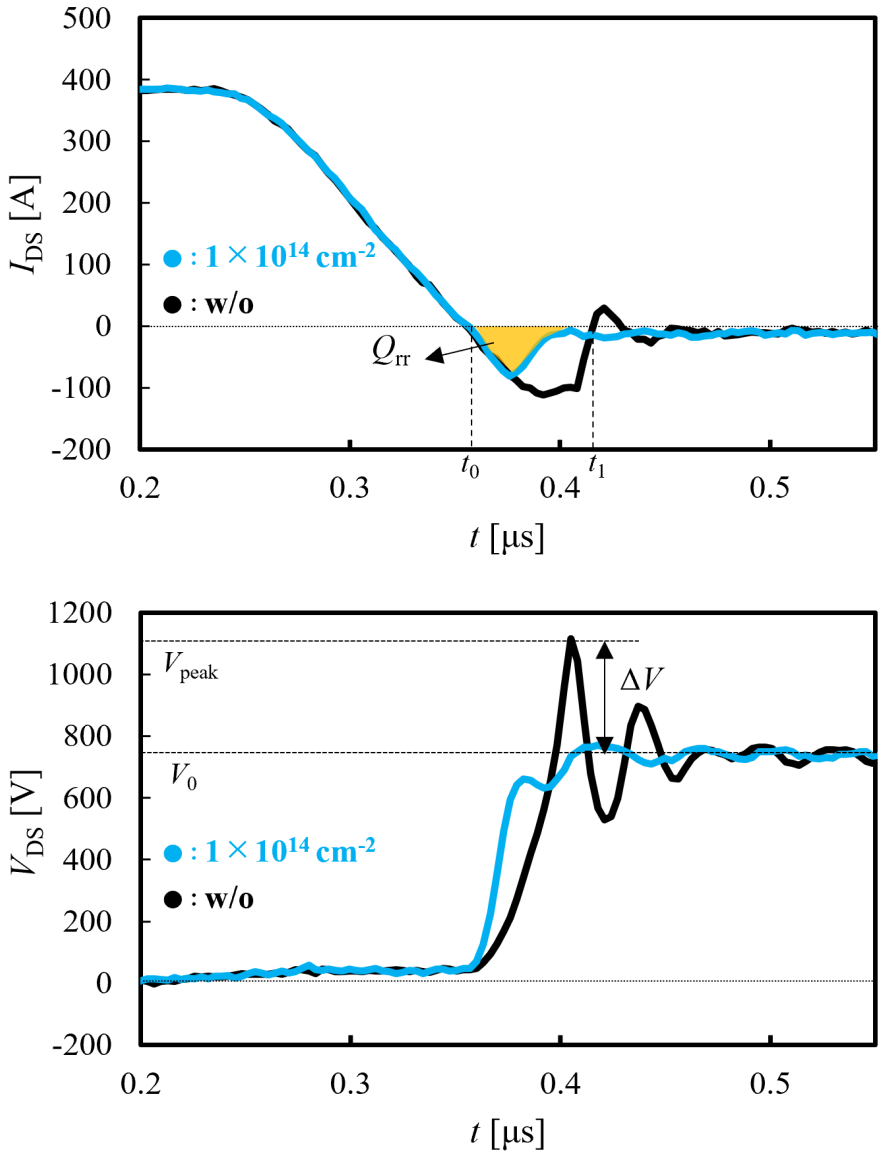

Fig. 8. Reverse recovery waveform of the body diode for (a) I_{DS} and (b) V_{DS}, respectively.

Table 1. Comparison of Q_{rr} and ΔV estimated from the reverse recovery waveform of the body diode without proton and with a proton dose of 1×10^{14} cm^{-2} (Figs. 8 (a) and (b)).

Proton	Q_{rr} [μC]	ΔV [V]
w/o	4.5	360
1×10^{14} cm^{-2}	1.9	14

where t_0 and t_1 are the times when I_{DS} becomes zero for the first time and the second time in the reverse recovery waveform, respectively. V_{peak} denotes the voltage that takes the largest value, and V_0 is the saturated voltage. As shown in Table 1, both Q_{rr} and ΔV successfully decreased by 58% and 96% with a proton dose of 1×10^{14} cm^{-2}, respectively. Our findings are that the implantation of proton not only has an effect on suppressing bipolar degradation but on reducing Q_{rr} and ΔV, which is a great advantage for reducing recovery loss and safe operation of the MOSFETs.

Now the origin of these effect is discussed here. Secondary ion mass spectrometry (SIMS) measurement revealed that implanted proton disappeared after the thermal annealing [3], which suggests that the existence of the hydrogen is not intrinsic. Point defect is known to be generated when the proton is implanted to an n-type 4H-SiC [6,7], whose typical one is $Z_{1/2}$ center ($E_c - 0.65$ eV) which acts as a lifetime killer [6-9]. Both experimental and theoretical research revealed that it is stable at high temperature [6,10]. We estimate that the recombination center derived from the point defect decreases the lifetime of carrier inside the epilayer, resulting in a decrease in Q_{rr}. Such a hypothesis can explain well the result of the 3rd quadrant characteristics. Proton implantation could reduce the lifetime of carrier and suppress conductivity modulation in the bipolar operation mode, which increases differential on-resistance. The disappearance of the temperature dependence, as shown in Fig. 6 (c), could be attributed to the suppression of the carrier increase at high temperatures via the recombination center. Although further study by using a deep level transient spectroscopy (DLTS) measurement would be needed, we estimate that the generation of the point defect derived from the proton implantation would be the key that reduce the bipolar degradation effect as well as obtaining favorable recovery characteristics of the MOSFET.

Summary

We fabricated huge numbers (about 4,000 chips) of proton implanted 4H-SiC MOSFETs, applied current stress to their body diodes and subsequently evaluated DC electrical characteristics and switching characteristics of them. We found that not only proton implantation has little influence except for the electrical characteristics as the 3rd quadrant characteristics on the DC characteristics but also it improves the switching characteristics. It could be related to the point defect introduced by proton implantation process. Evaluation of the on-resistance of the MOSFETs before and after the current stress on the body diode revealed that the increase of the resistance due to the expansion of the SFs could be suppressed. Establishing a suitable proton implantation condition will surely open the way for its introduction to the future mass production of the bipolar-tolerant and reliable SiC MOSFETs.

Acknowledgement

We would like to thank H. Hatta of Mitsubishi Electric Corp. for his fruitful discussion and technical support of measurement.

References

[1] T. Tawara, T. Miyazawa, M. Ryo, M. Miyazato, T. Fujimoto, K. Takenaka, S. Matsunaga, M. Miyajima, A. Otsuki, Y. Yonezawa, T. Kato, H. Okumura, T. Kimoto and H. Tsuchida, J. Appl. Phys. **120**, 115101 (2016).

[2] M. Kato, O. Watanabe, T. Mii, H. Sakane and S. Harada, Sci. Rep. **12**, 18790 (2022).

[3] S. Harada, T. Mii, H. Sakane and M. Kato, Sci. Rep. **12**, 13542 (2022).

[4] M. Kato, S. Harada and H. Sakane, Jpn. J. Appl. Phys. **63**, 020804 (2024).

[5] M. Skowronski and S. Ha, J. Appl. Phys. **99**, 011101 (2006).

[6] T. Dalibor, G. Pensl, H. Matsunami, T. Kimoto, W. J. Choyke, A. Schöner and N. Nordell, Phys. Status Solidi A **162**, 199 (1997).

[7] T. Dalibor, C. Peppermüller, G. Pensl, S. Sridhara, R. P. Devaty, W. J. Choyke, A. Itoh, T. Kimoto and H. Matsunami, Inst. Phys. Conf. Ser. **142**, 517 (1996).

[8] P. B. Klein, B. V. Shanabrook, S.W. Huh, A. Y. Polyakov, M. Skowronski, J. J. Sumakeris and M. J. O'Loughlin, Appl. Phys. Lett. **88**, 052110 (2006).

[9] K. Danno, D. Nakamura and T. Kimoto, Appl. Phys. Lett. **90**, 202109 (2007).

[10] C. Zechner, M. Tanaka, K. Shimai, N. Zographos, S. Kanie and S. Tsuboi, J. Appl. Phys. **132**, 035702 (2022).